CONTRACT REPORT NO. 3-91

# STUDY OF THE DYNAMIC STRESS-STRAIN AND WAVE-PROPAGATION CHARACTERISTICS OF SOILS

Report 2

## CORRELATION OF STRESS-STRAIN AND WAVE-PROPAGATION PARAMETERS IN SHOCK-LOADED DRY SANDS

by

W. L. Durbin

November 1964

Sponsored by

Defense Atomic Support Agency

Conducted for

U. S. Army Engineer Waterways Experiment Station
CORPS OF ENGINEERS
Vicksburg, Mississippi

Under

Contract No. DA-22-079-eng-373

by

United Research Services, Inc.
Burlingame, California
(URS 637-15)

CONTENTS

Contents (Continued)

ILLUSTRATIONS

Illustrations (Continued)



TABLES

## ABSTRACT

Wave propagation studies conducted on laterally confined columns of three granular materials which exhibit nonlinear stress–strain behavior are described. Under these conditions, axial and lateral stresses and strains, wave velocities, and particle velocities measured at points along the column are reported. A new technique for measuring free-field displacements without physically contacting the soil is also described.

A correlation between the moduli computed from the stress wave velocity, particle velocity, and the secant drawn to the stress–strain curve is presented. Relationships between stress, strain, wave velocity, and particle velocity are shown to be such that if any two of the parameters are known, the other two may be determined. Comparison of the data is made with the Hertzian theory relating confining stress to wave velocity or constrained modulus.

The difference between a stress–strain curve for a static loading and the unique relationship that exists between stress and strain for shock loadings is presented.

Correlations are presented showing good agreement between axial stress and strain data taken after passage of the incident wave and those taken after the passage of the reflected wave.

Several interesting though preliminary observations on stress precursors resulting from initial axial stresses are presented. Based on these observations, an explanation is presented for the disparity between moduli based on constrained compression tests and those back-figured from seismic velocities.

# Section 1
# INTRODUCTION

This study is part of a program to extend knowledge of the behavior of soil under dynamic loading conditions. The current effort has been undertaken to examine those aspects of the behavior of granular material that are uniquely associated with propagating stress waves wherein inertial properties play a role. The program, initiated by the Defense Atomic Support Agency (DASA) is currently under sponsorship of the U.S. Army Engineer Waterways Experiment Station (WES).

One of the most difficult decisions for the soil mechanics engineer is the proper choice of modulus to define the stress–strain behavior of the soil, i.e., a wide discrepancy exists between a modulus obtained from confined compression tests and one back-figured from seismic velocities. This problem is not unique to the design of protective construction; however, it is much more serious in view of the high stresses and dynamic effects resulting from blast loadings.

The aim of this report then, is to present experimental evidence of the basic behavior of soils that will aid the engineer in making his judgment as to the modulus of the materials he is working with, as well as provide a means of predicting wave velocities and particle velocities from the stress–strain response. In doing so, other observations of wave propagation

phenomena seen in columns of granular materials subjected to impulsive loads that are step-shaped stress pulses will be presented. Further, it is hoped to clarify the meaning of a stress–strain curve for impulsive loadings with very fast rise times.

This work was done under the technical guidance of Mr. H. G. Mason, Chief of the Soils and Structural Mechanics Group of URS. Direct supervision was provided by Mr. J. V. Zaccor, Project Manager. Special thanks go to Mr. D. F. Walter, who conducted most of the tests.

## Section 2
## EXPERIMENTAL FACILITIES

The equipment used in this study, and the techniques employed, are those developed at URS under contract with the Defense Atomic Support Agency and have been described in greater detail in earlier reports (Refs. 1, 2, and 3).

### TEST SAMPLE

In this study, a sample column 12.85 in. long by 1.5 in. in diameter was confined laterally by a relatively frictionless fluid annulus enclosed by a thick-walled Plexiglas cylinder (Fig. 1). Photographs of the apparatus can be found in Report No. 1 of this series. The purpose of the fluid annulus was to provide minimum resistance to axial displacement while maintaining maximum resistance to lateral motion. In this way, plane-wave conditions could be approximated.

There are many factors contributing to volume changes in the surrounding fluid, including those resulting from the fact that the fluid is not truly incompressible. However, it was observed that the major portion of these volume changes seemed to be confined to the upper portion of the column, such that beyond some depth the fluid compressibility was the dominant factor in allowing lateral displacement. Since there are a number of plates and seals at the top of the column that could be a source of volume changes, it is likely that as the wave enters the sample, the lateral motion due to these changes takes place immediately. Once the wave front passes this portion of the sample, these changes

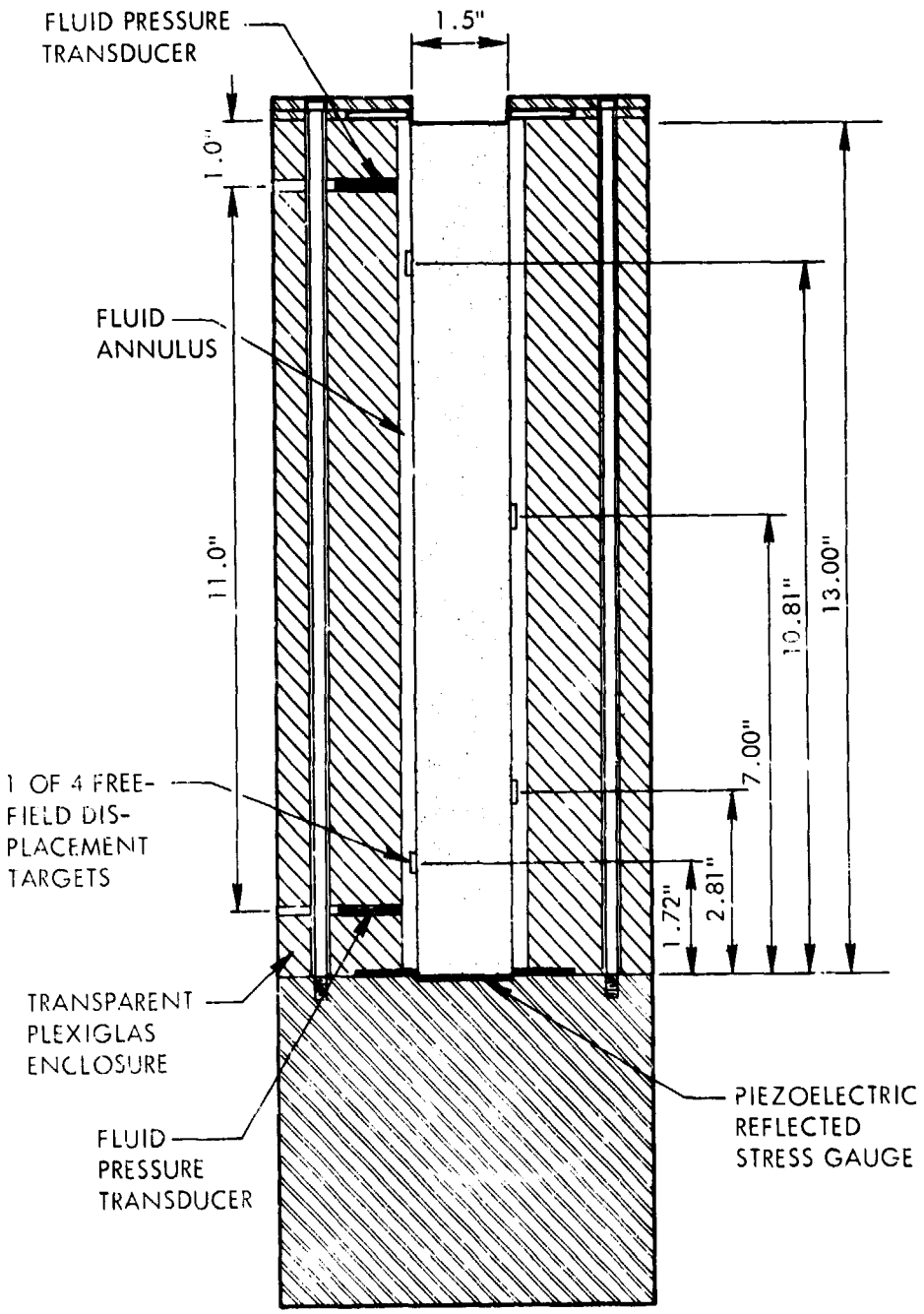


Figure 1. Confined Compression Apparatus

have occurred, and lateral displacements result primarily from the bulk compressibility of the fluid. Lateral displacement measurements indicated that radial strains in this lower region were on the order of 1.5 microstrain* per psi of axial load. The initial tests in this study were conducted on 20−30 Ottawa sand for the following reasons. First of all, since a great deal of testing has been conducted on Ottawa sand, its properties were well defined and, consequently, the use of it would aid in evaluating the test set-up. Secondly, it could be placed at the desired densities by methods developed in an earlier program and, thus, eliminate the need for additional placement studies at this time. Lastly, since this sand comes close to being a mono-size, spherical aggregate, it was expected that it would show the best correlation with any theory based on a dense packing of equi-radii spheres.

The description of two other sands furnished to URS by WES and used in this study is as follows:

1. Sand no. 1 was obtained from a natural deposit in Warren County near Culkin, Mississippi, and is locally called Cooks Bayou sand. This material is a clean, fine, uniform sand with predominantly subrounded particles and is used commercially as a masonry sand.
2. Sand no. 2 was originally obtained from a natural deposit along the Big Black River in Warren County near Yokena, Mississippi, is locally called Reid Bedford Model sand, and was used in a hydraulic model study. This sand is classed as a uniform, fine sand with particles that are partly subangular and partly subrounded.

Some of the physical properties of these sands are summarized in Fig. 2.

Because of the relatively large number of tests required to accurately define a stress−strain relationship, only one placement

---

* 1 microstrain = 1 microinch per inch

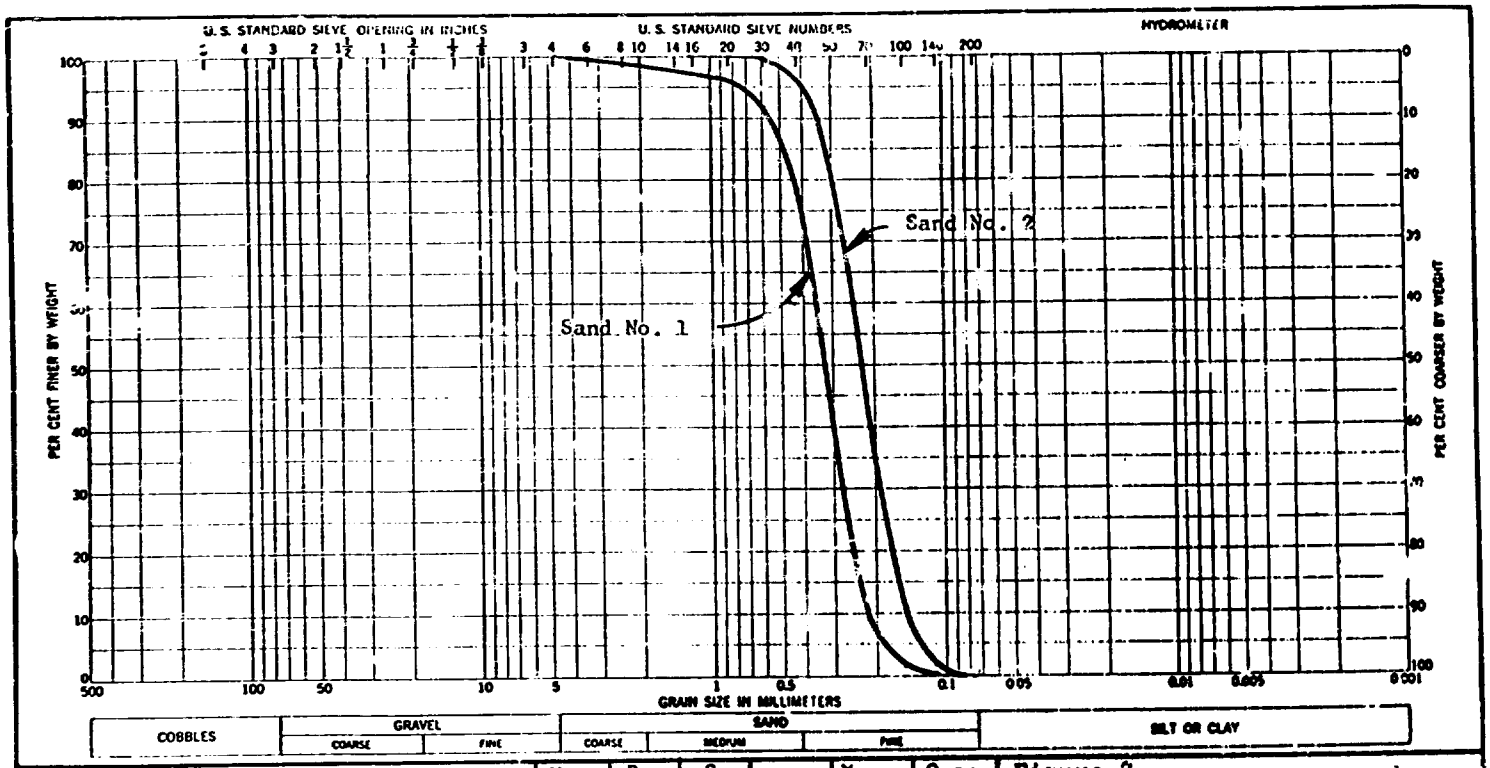


| Sample No. | Local Name | Nat w % | $D_{50}$ (mm) | $C_u$ | $\gamma_{d\ max}$ (pcf) | $\gamma_{d\ min}$ (pcf) | Quan rep. |
|---|---|---|---|---|---|---|---|
| Sand No. 1 | Cooks Bayou Sand | 0.1 | 0.32 | 1.7 | 110.8 | 93.3 | 75 lb |
| Sand No. 2 | Reid Bedford Model | 0.1 | 0.23 | 1.6 | 104.2 | 87.2 | 75 lb |

**Figure 2.**
**Physical Properties of Sand Samples**

**Furnished URS by WES**

**March 1964**

method was used for both the Cooks Bay sand ($\gamma$ = 107.5 pcf, RD ~ 80%) and the Reid Bedford Model sand ($\gamma$ = 98.5 pcf, RD ~ 70%). For the 20−30 Ottawa sand, two different placement procedures were used, one which yielded a density of 110.0 pcf (RD ~ 90%) and the other a density of 105.5 pcf (RD ~ 60%). A brief summary of sample placement is given in Appendix B.

## DYNAMIC LOADER

The samples are loaded through a piston by air loadings generated in a modified shock tube (Ref. 1). Direct air loadings on the piston as high as 2000 psi, with rise times from 10 to 100 μsec, are possible. Slower rates of loadings can be achieved through a system of orifices that reduce the rate at which the pressure is applied to the piston. For the fast loadings, the actual rise time of the stress in the soil is lengthened because of the mass of the piston. The rise time at the input-end of the sample varies from 700 μsec at the lower stress levels to 150 μsec at higher stresses. The rise time is somewhat reduced as the stress wave becomes a stable shock*. The fluid surrounding the sample is sealed from the air loading so that the lateral pressure is generated by the axial loading on the soil.

## MEASUREMENTS

The measurements recorded in this series of tests consisted of axial and lateral stresses and displacements, all measured as a function of time. Wave velocities and particle velocities were obtained from these measurements.

---

* For a brief discussion of shock phenomena in soils see Ref. 4, Appendix B.

## Stress Measurements

A piezoelectric crystal, 1-1/2 in. in diameter, located at the base of the sample column, is used to measure axial stress. When shock loadings are applied, a reflection takes place as the wave strikes the crystal, and consequently, the base gauge reads the reflected stress rather than incident pressure. In the current study, there was no means of bringing lead wires out of the sample cavity, so no free-field stress gauges were used. However, lateral pressures were measured and found to be relatable to the axial stress in the soil so that they may be used to infer the free-field incident axial stress (Ref. 4, Appendix C). These lateral pressures were monitored by Kistler pressure transducers located in the wall of the enclosure, 1 in. from either end (see Fig. 1).

## Displacement Measurements

The axial displacement of the input end of the sample was measured by a capacitance-type gauge manufactured by Photocon Research Products. In addition, axial displacements of the targets appended to the membrane at various points along its length (Fig. 1) were recorded by Optron 701 optical displacement followers. A discussion of the operation of the 701 optical displacement followers as well as the 680 electro-optical trackers is given in Appendix A.

In making these measurements, it was assumed that the membrane remained in one-to-one correspondence with the sand particles, and displacements of the targets would, therefore, be representative of the sample motion. Two Optron 680 followers loaned to

URS by the Optron Corporation provid[illegible] some information to support this assumption. In two tests a black line was painted on the inside of the membrane near the input end of the column, and a layer of colored Ottawa sand grains was placed adjacent to it. (This location was selected because relative displacements of sample and membrane should be a maximum there.) One instrument was then locked on the line and the other was locked on the layer of colored sand grains. In one test there was no measurable differential displacement between the two stations, and in the other test there was only a small relative displacement (amounting to 2.5 percent error in total column strain). After determining that the membrane and the sand grains remained in one-to-one correspondence, targets were appended to the membrane. However, it was discovered that the targets had an inertial lag due to the extremely fast loading of the sample and the mass and configuration of the target.

In this test series it was only possible to record lateral displacements for the lower two inches with the 701 Optrons because of the necessity of having a reflective surface. However, with the installation of the 680 trackers, lateral displacement measurements should be possible at any point on the column since these trackers "lock-on" the edge of the column itself. (See Appendix A for further detail.)

Velocity Measurements

Particle Ve[illegible]ity measurements were obtained from the slope of the displacem[illegible]ime traces, while the wave velocity was obtained

from the quotient of the sample length divided by the travel time between the displacement sensor at the surface and the reflected-stress gauge at the base.

The above information was recorded on Tektronix 502 Dual-Beam Oscilloscopes. As many as 12 channels of information were required to describe a single test.

# Section 3
# DISCUSSION OF RESULTS

## STRESS – STRAIN DATA

### Background

Before discussing the results, it is imperative that one understand just what is meant by a "stress – strain curve" for impulsive loadings. Clearly, if a loading is very slow, so that the rise time is many times greater than the travel time through the sample, the stress – strain relationship can in most instances be obtained by simply recording, at a common time, the load and the deformation over any convenient gauge length. This procedure is valid whenever the entire sample is essentially uniformly stressed at all times throughout the loading period, as is the case for static loadings. Some investigators have also applied this procedure in their studies of dynamic loading conditions even when it has not been valid. For example, in the case of shock loadings or loadings with fast rise times*, a common time plot is not satisfactory, since the sample is not uniformly stressed except at certain unique instances in time. To simply ignore the phase difference in measurements and record the stress and strain at a common time would lead to errors, since strain is measured over a finite length of sample and stress at a point.

---

* Whitman has suggested the following criterion for the lower limit of rise time: $t_L > 25\ L/C$ where $t_L$ = rise time, L = sample thickness, C = wave velocity. (See Ref. 8.)

This fact is illustrated by comparing the two traces in Fig. 3, which were obtained by plotting (at common times) on the oscilloscope stress measured at a fixed end of a sample versus displacement at the other end. In Fig. 3A, a concave-upward stress−strain trace is recorded for a slow loading and unloading. Figure 3B shows a similar trace, i.e., stress versus displacement at common times, for a shock loading. This could not possibly be construed as a stress−strain curve for the material. Properly interpreted, it is apparent that slightly more than half of the total displacement that is to occur (in fact, all that results from the incident stress wave) has taken place at the upstream gauge station by the time the incident stress reaches the stress gauge at the base. (This is the first time at which the soil in the gauge length becomes uniformly stressed.) Figure 3C shows how a stress−strain trace would look (hypothetically) if the stress had been measured at the input end of the sample as had the displacement. In this case virtually all the stress would appear to occur before a significant amount of straining took place*. Obviously, neither Fig. 3B nor 3C, per se, represents an accurate "stress−strain" relationship.

To obtain the correct relationship between stress and strain, it is necessary to determine the strain that corresponds to a uniformly stressed sample, and for step-shaped shock loadings this requires a separate test for each stress level. Since the

---

* For certain combinations of rise time and travel time through the sample, this could be especially dangerous since, although stress and strain would appear to occur at the same time, they would actually be out of phase, thus indicating an erroneous relationship that would not be obvious.

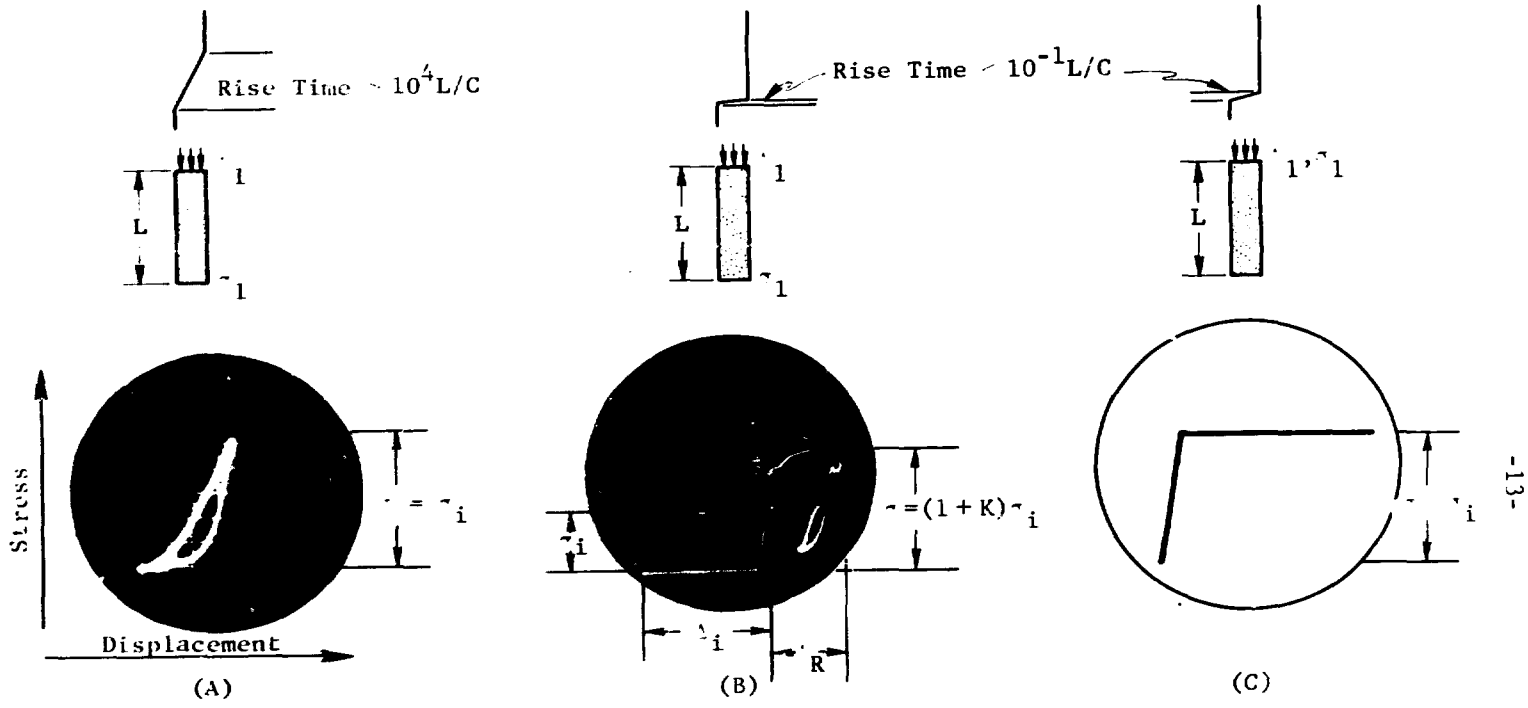


NOTE:

C = Wave velocity
K = Reflection Factor
= Peak stress
= Displacement due to
$\sigma_i$ = Incident stress
$_R$ = Displacement due to the reflected stress

Figure 3. Stress—Displacement Traces Showing the Effect of Variation in Rise Time and Gauge Location

loading is a step pulse of infinite duration, the relationship between stress and strain can be obtained for any gauge length simply by measuring the relative displacement over that gauge length at the time the incident wave first reaches the base. Furthermore, it was found (Refs. 2, 4) that the peak displacement could be associated with the peak reflected stress as another condition of a uniformly stressed sample (Fig. 4), therefore two stress–strain points can be obtained from each test. This agreement implies that a reflected wave of magnitude $(K - 1)\sigma_1$* moving into material with a particle velocity, v, generated by the incident stress, $\sigma_1$, has the same effect as the application of a stress wave of magnitude $(K - 1)\sigma_1$ moving into a sample with no particle velocity.

Free-Field Displacements

As mentioned earlier, the axial displacements were measured at several points along the length of the column in addition to that measured at the surface. Most of these free-field displacements were measured at 7 in. and 1.7 in. from the base. Here again, incident values are plotted as well as peak reflected stresses and displacements (Fig. 5). The fact that the stress–strain curve (curve A, Fig. 5) based on free-field displacements did not agree with that measured at the surface (curve B, Fig. 5) was anticipated, the reason being that lateral expansion due to volume changes, other than those due to the bulk compressibility of the fluid, were expected to take place at the top portion of the sample and result in greater axial displacements than would occur in the lower portion of the sample.

---

* Where K is the reflection factor (Ref. 4, Appendix C).

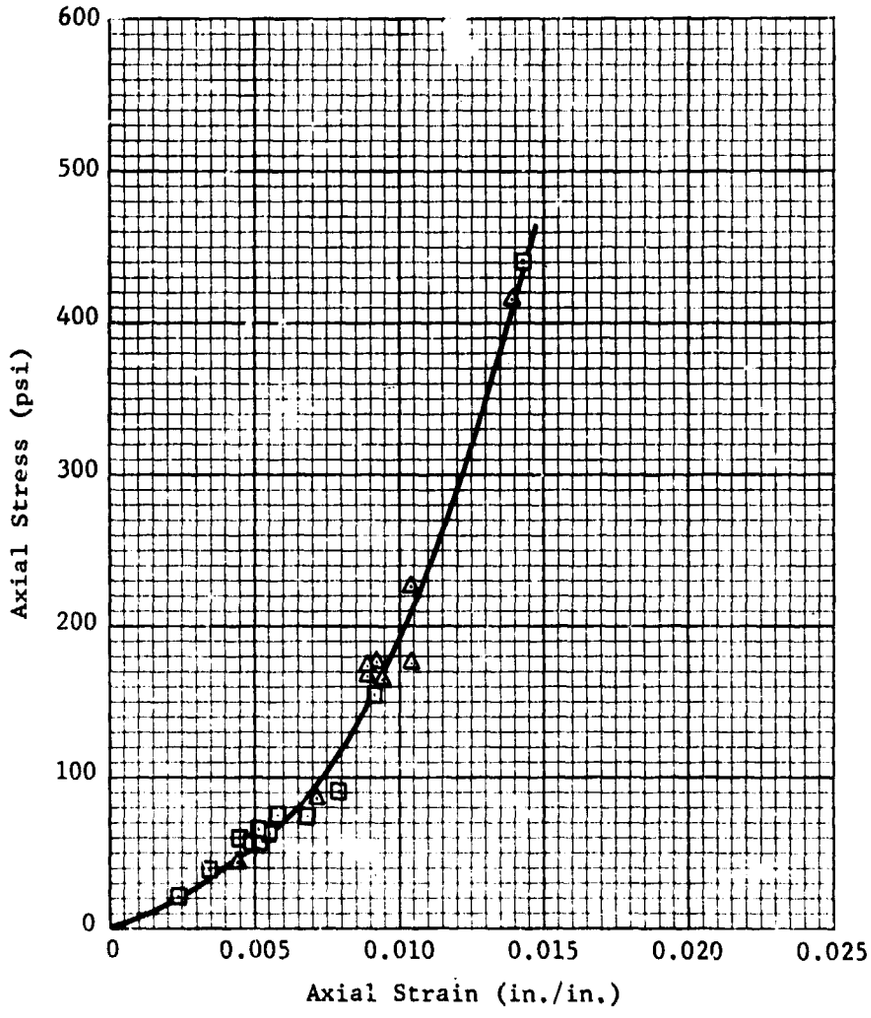


Legend:

- ☐ Incident stress versus strain for 12.8-in. gauge length
- △ Peak reflected stress versus strain for 12.8-in. gauge length

Figure 4. Stress–Strain Curve in 20–30 Ottawa Sand As Measured at the Surface $\gamma$ = 110.0 pcf (RD ≈ 90%)

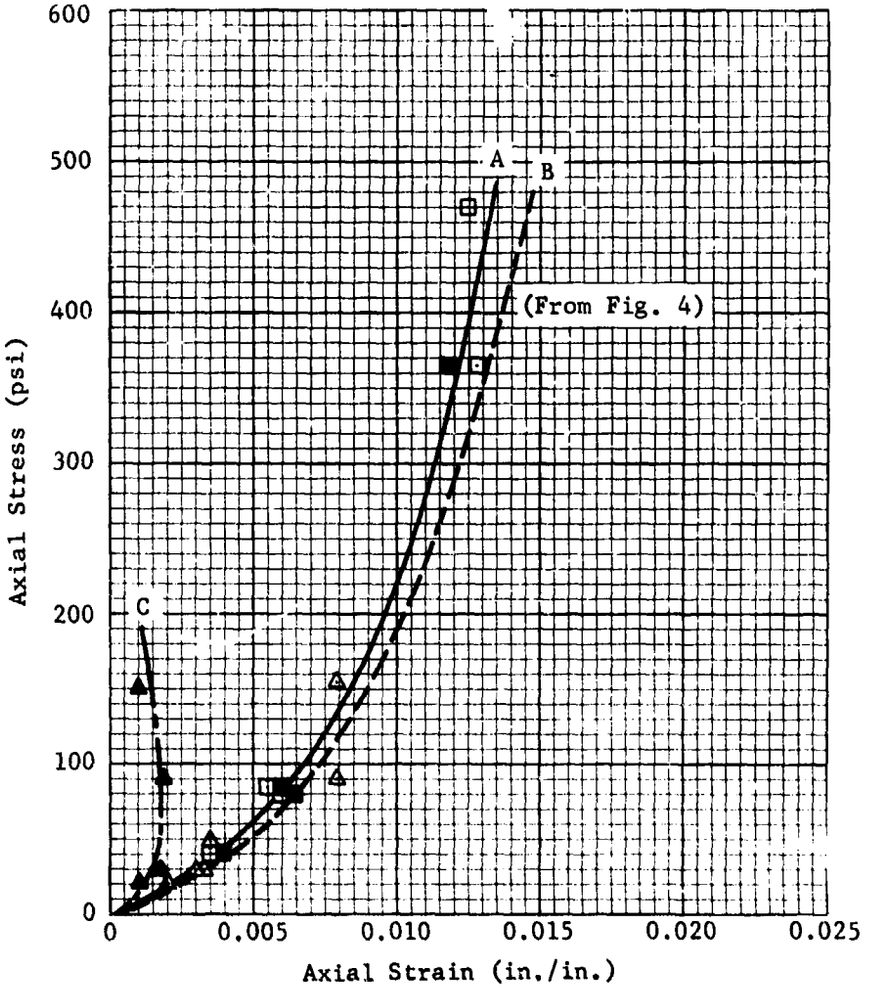


Legend:

△ Incident stress versus strain for 7.0-in. gauge length
□ Peak reflected stress versus strain for 7.0-in. gauge length
▲ Incident stress versus strain for 1.7-in. gauge length
■ Peak reflected stress versus strain for 1.7-in. gauge length

Figure 5. Stress–Strain Curves in 20–30 Ottawa Sand for Various Sample Lengths $\gamma$ = 110.0 pcf (RD ≈ 90%)

To verify this assumption, lateral displacement measurements were made with the Optron 701 displacement followers near the bottom target. No lateral expansion could be resolved under an incident stress of 100 psi and, consequently, must have been less than the resolution of the equipment, which is on the order of 150 microinches. However, it was evident that measurable radial displacements were occurring at the top of the sample.

The obvious discrepancy of the stress–strain curve based on the data for the incident stress and strain at the bottom target (Fig. 5, curve C) was not too surprising in view of the inertial effects that appended targets would likely have*. The fact that the peak reflected stress versus peak strain, for the bottom target, which occurs later in time, agrees with the data for the other stations supports the contention that the discrepancy is due to inertial lag. Nevertheless, it was considered possible that the relationship between inertial lag of target and true sample motion might be evaluated and a correction applied. However, the extremely critical nature of timing the stress waves makes this currently unattractive, in that it becomes a sizable study in itself.

---

* Since the displacement in question is determined at the time the stress wave first reaches the base, a delay in the start of the motion of the target will result in less strain being recorded at the critical time. Since the stress-wave velocity increases with pressure and, consequently, the time it takes the stress wave to travel from the target to the base decreases, it is possible to have the apparent strain decrease as the pressure level increases, producing the unusual stress–strain curve in Fig. 5, curve C.

The fact that there was no apparent dis arity for the target 7 in. above the base could be explained by either of the following reasons. First, the lag time could be such a small portion of the travel time through the 7 inches of sample that the discrepancy is not noticeable. Secondly, it is possible that the target has had time to "catch up" with the soil. This would imply that the target velocity, once the target began moving, was actually greater than that of the sand.

The measured displacements of the lower 7 inches of the sample column were used in order to obtain stress–strain curves for comparison with the wave velocity and particle velocity. A sample length was thus obtained that had no measurable lateral displacement. In addition, the stress was fully shocked up for the total gauge length. The particle velocity measurements used in the comparison were also obtained from the target 7 in. above the base. The wave velocity measurements were based on the travel time through the entire sample, and this was assumed to be representative of the average velocity at the middle of the sample. As a result, all measurements were assumed to correspond to the response at a common point, the middle of the sample.

The stress–strain curves in the various sands are presented in Fig. 6. For the most part, the variation in strain is less than ±10 percent from the mean curve drawn through the points for a given material.

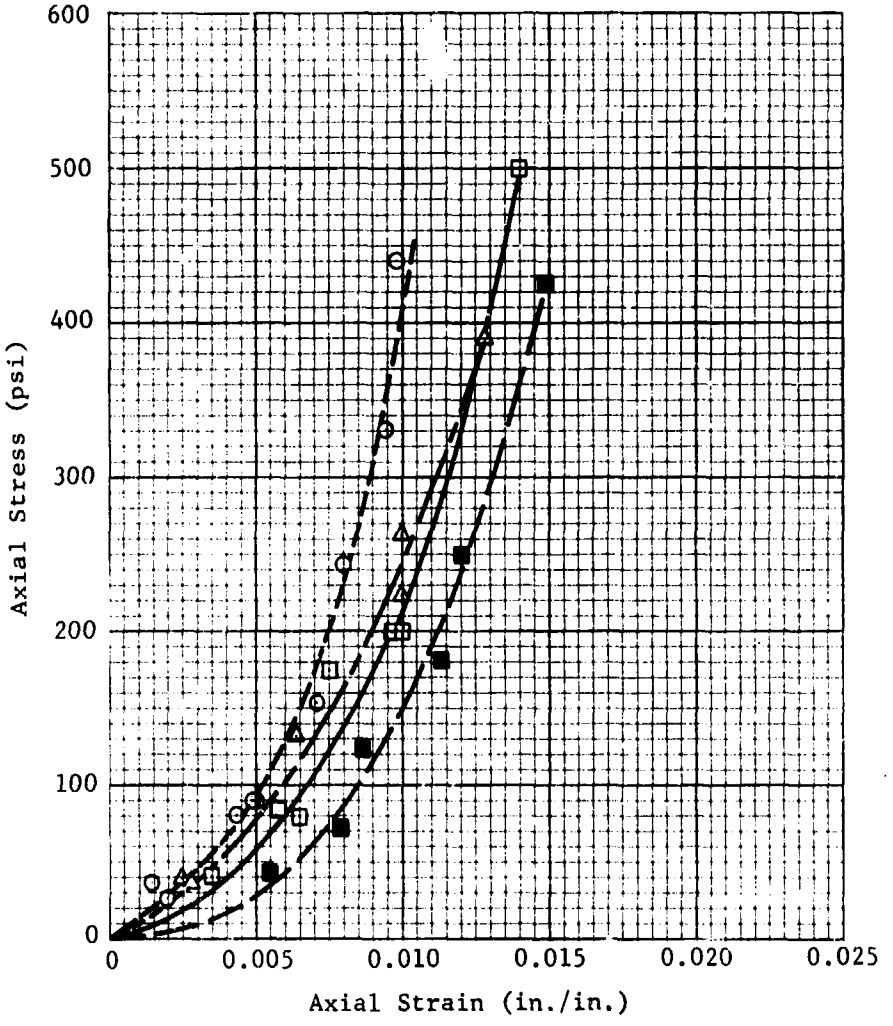


Legend:

| | | |
|---|---|---|
| □ | 20−30 Ottawa sand | γ = 110.0 pcf (RD ≃ 90%) |
| ■ | 20−30 Ottawa sand | γ = 105.5 pcf (RD ≃ 60%) |
| ○ | Cooks Bayou sand | γ = 107.5 pcf (RD ≃ 80%) |
| △ | Reid Bedford Model sand | γ = 98.5 pcf (RD ≃ 70%) |

Figure 6. Stress−Strain Curves for Granular Media

## WAVE VELOCITY DATA

The wave velocity is plotted as a function of axial stress in Fig. 7 for the various sands tested. Considerable variation was obtained for Cooks Bayou sand, and it was difficult to determine the best fit of all points. For the other three curves the variation is within ±10 percent.

## PARTICLE VELOCITY DATA

Particle velocities also seemed to be relatable to overpressure, as shown in Fig. 8. For the looser placement of 20−30 Ottawa sand ($\gamma$ = 105.5 pcf) the results did not follow the same relationship exhibited by the other sands. Since the displacements were quite large, it is possible that they actually exceeded the linear range of the tracker's output. Consequently, the particle velocity measurements in the looser arrangement of 20−30 Ottawa sand were not used in the comparison of moduli, although the data were presented in Fig. 8.

## CORRELATION OF MODULI

Since the propagating waves appear to be shock waves, the wave velocity is related to the secant modulus and the particle velocity by the following equations:

$$M = \sigma_1/\varepsilon_1 = \rho_o C_{\sigma_1}^2 = \sigma_1^2/\rho_o v_1^2 \qquad (1)$$

where: $M$ = secant modulus

$\rho_o$ = mass density

$\sigma_1$ = axial stress

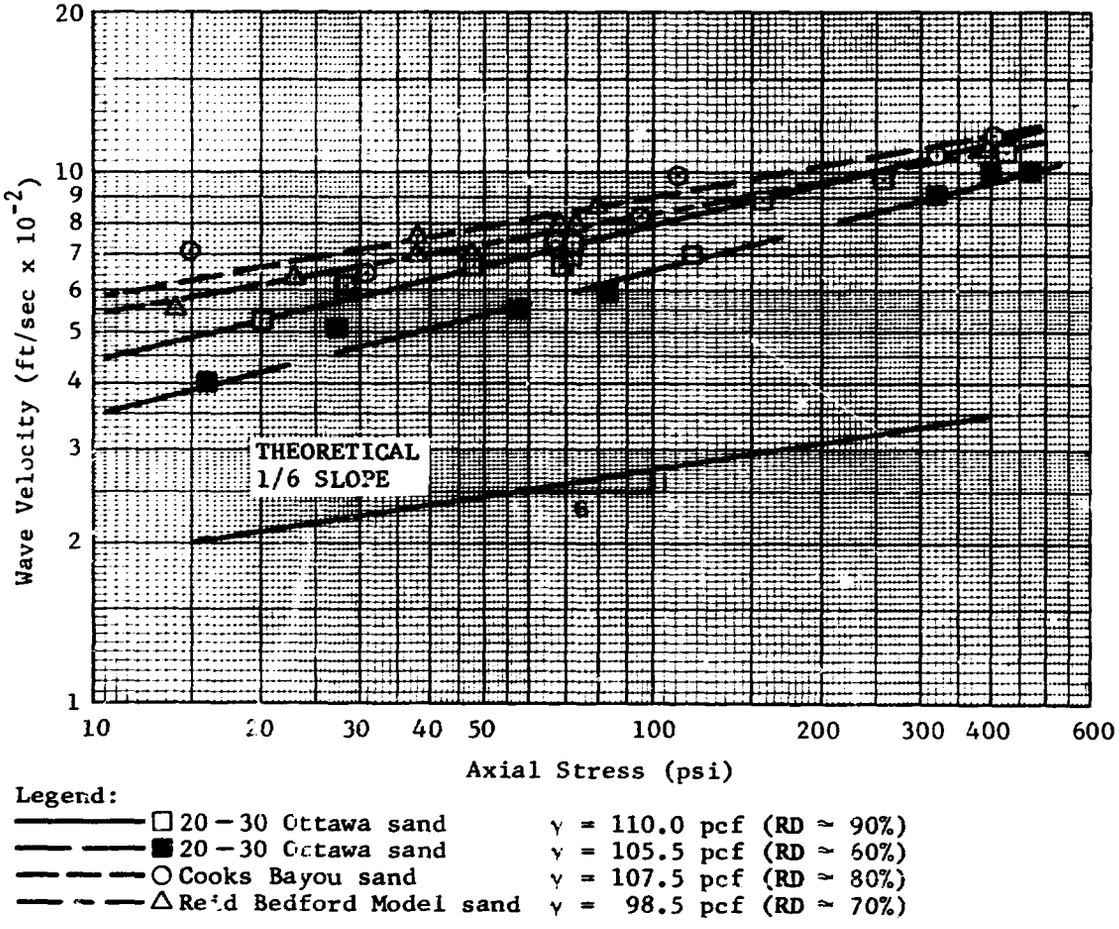


Figure 7. Wave Velocity Versus Axial Stress in Granular Media

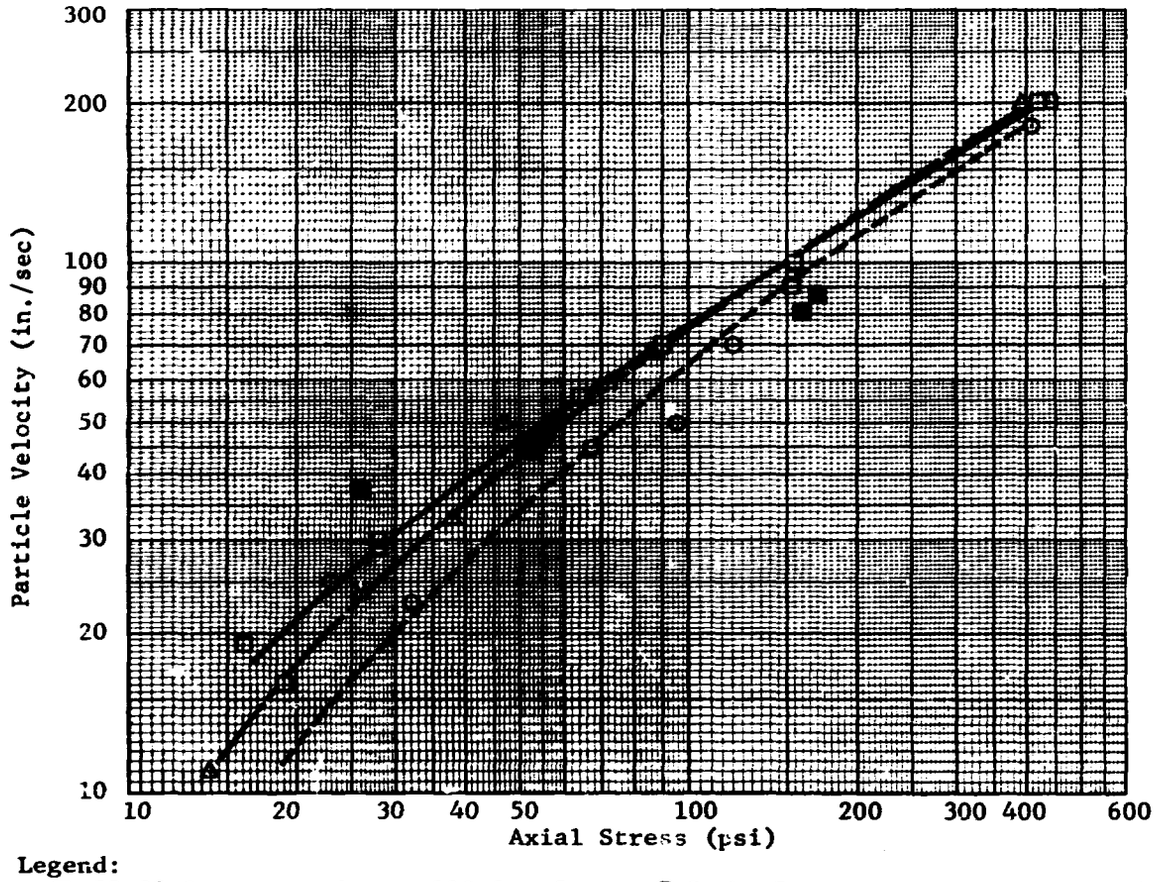


Legend:

□ 20-30 Ottawa sand $\gamma$ = 110.0 pcf ○ Cooks Bayou sand $\gamma$ = 107.5 pcf

■ 20-30 Ottawa sand $\gamma$ = 105.5 pcf △ Reid Bedford Model sand $\gamma$ = 98.5 pcf

Figure 8. Particle Velocity Versus Axial Stress in Granular Media

$\varepsilon_1$ = axial strain
$C_{\sigma_1}$ = velocity of wave (of stress level $\sigma_1$)
$v_1$ = particle velocity

The modulus values plotted in Figs. 9 through 12 were calculated using Eqs. (1) and the curves in Figs. 6 through 8.

The correlation between the moduli obtained from wave velocity, particle velocity and the stress–strain curve is encouraging. The biggest disparity is found for the modulus based on particle velocities, chiefly at low stress levels*. Nevertheless, the agreement between the wave velocity modulus and that obtained from the secant to the stress–strain curve appears excellent in view of the disparities gener ly found in comparing such measurements.

COMPARISON WITH THEORY

Theory predicts the proportionality of the wave velocity to the sixth root of the confining pressure (Ref. 5), at least for a dense packing of equi-radii spheres subjected to small stress changes. Since in the URS test apparatus the lateral "confining" pressure is generated by the axial stress (and the

---

* This disparity could also be explained by the argument given earlier, i.e., that the target travels at a greater velocity than the sample in order to "catch up" with it.

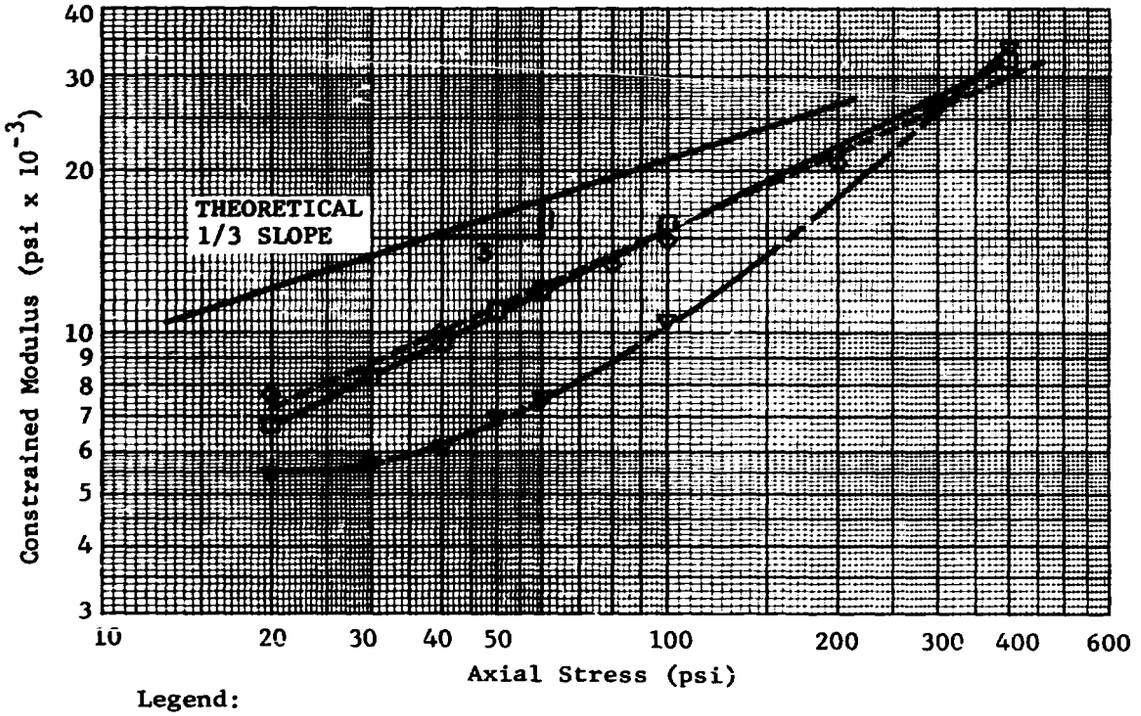


Legend:

◇ Secant modulus from stress-strain curve
□ Modulus from wave velocity (curve A, figure 7)
▽ Modulus from particle velocity (curve A, figure 8)

Figure 9. Constrained Modulus Versus Axial Stress in 20—30 Ottawa Sand $\gamma$ = 110.0 pcf (RD ≃ 90%)

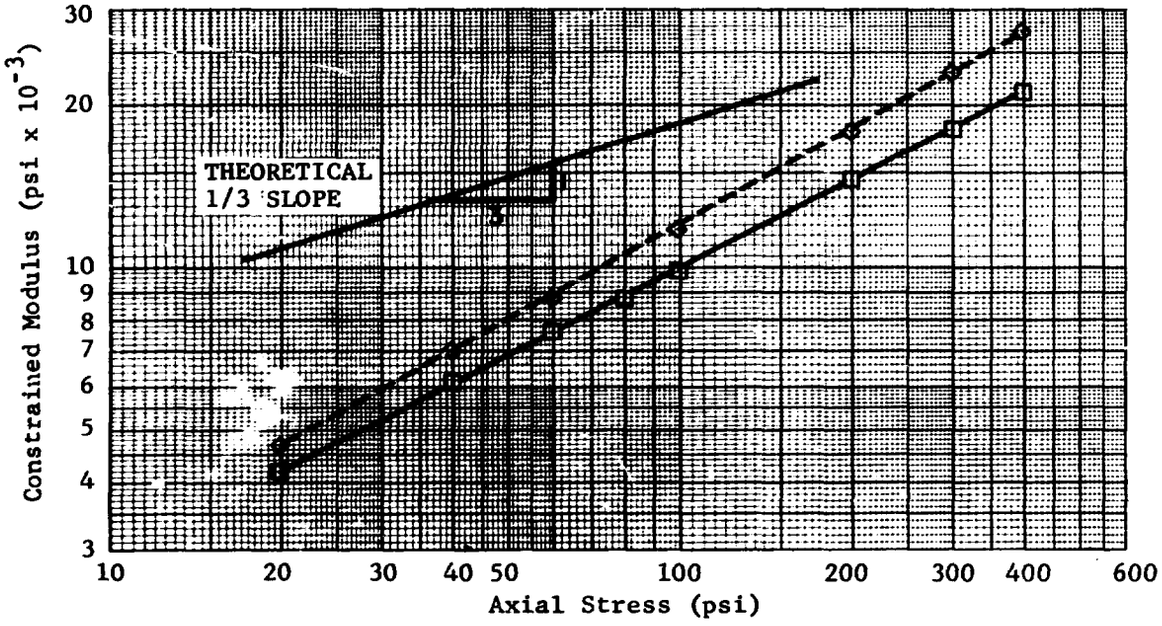


Legend:

◇ Secant modulus from stress-strain curve

□ Modulus from wave velocity (curve B, figure 7)

Figure 10. Constrained Modulus Versus Axial Stress in 20–30 Ottawa Sand $\gamma$ = 105.5 pcf (RD ≃ 60%)

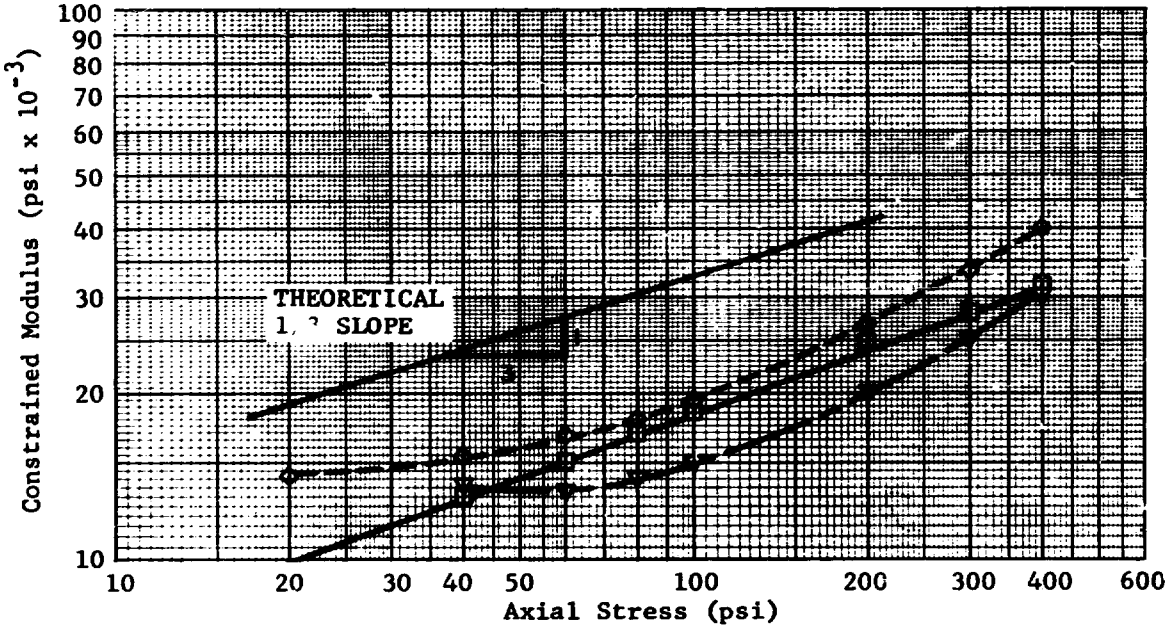


Legend:

◇ Secant modulus from stress-strain curve
□ Modulus from wave velocity (curve C, figure 7)
▽ Modulus from particle velocity (curve C, figure 8)

Figure 11. Constrained Modulus Versus Axial Stress in Cooks Bayou Sand $\gamma$ = 107.5 pcf (RD ≃ 80%)

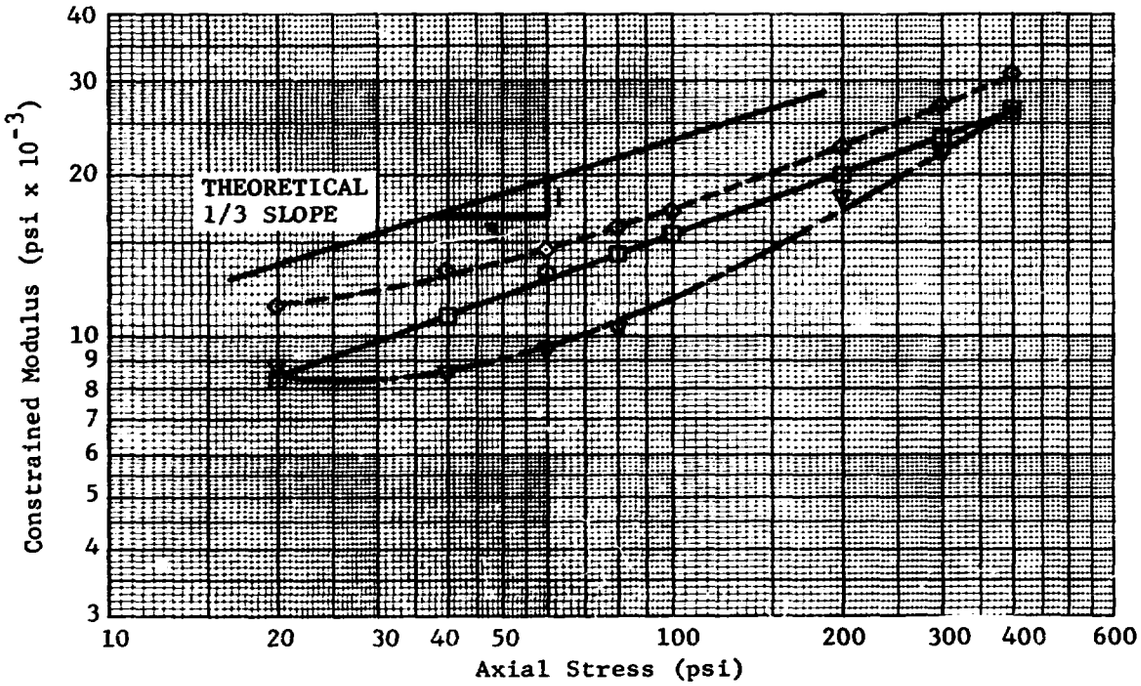


Legend:

◇ Secant modulus from stress-strain curve
□ Modulus from wave velocity (curve D, figure 7)
▽ Modulus from particle velocity (curve D, figure 8)

Figure 12. Constrained Modulus Versus Axial Stress in Reid Bedford Model Sand $\gamma$ = 98.5 pcf (RD ≃ 70%)

ratio of lateral to axial stress is essentially a constant independent of the stress level), it is reasonable to expect the wave velocity to vary as the sixth root of both the axial and lateral stresses.

In comparing the curves in Fig. 7, it is evident that this relationship does not hold for all the materials tested. It was anticipated that the dense packing of 20 − 30 Ottawa sand would be most likely to show agreement with theory since 20 − 30 Ottawa sand comes closest to satisfying the conditions. However, it is apparent that the wave velocity for 20 − 30 Ottawa sand increases at a faster rate than predicted, and the rate appears to be nearly independent of density. On the other hand, both Cooks Bayou sand and Reid Bedford Model sand show better agreement with the theory. Although the loading conditions in effect were not the same as those specified by the Hertzian theory, presented in Ref. 5, the correlation is quite good in view of the fact that even for tests on steel balls, the trend was for the wave velocity to increase faster than predicted by the one-sixth law (Ref. 5). Investigators have also observed this same sort of relationship between wave velocity and confining stress in other test devices (Ref. 7).

Similarly, from the relationships in Eqs. (1), it is obvious that the moduli should vary as the cube root of the applied pressure. This comparison is shown on Figs. 9 through 12.

STRESS PRECURSOR

The analysis of the data mentioned above also revealed a low-stress precursor (Fig. 13A)*. In order to determine the overall effect of an initial overburden, a few special tests were conducted on 20−30 Ottawa sand at a density of 110 pcf. In the first of these tests, an axial static overpressure of 60 psi was placed on the sample prior to applying the 30-psi dynamic increment. It was anticipated that the larger resultant confining pressure would produce a larger magnitude precursor with a faster wave velocity than the tests with virtually no initial axial overpressure, since, as mentioned, the wave velocity is proportional to the confining pressure, and in this device the "confining" pressure is generated by the total axial load. The magnitude did increase from approximately 1 psi to about 10 psi, and the velocity increased from about 1000 ft/sec to 2100 ft/sec. Two more tests of this nature were conducted. The data from all three tests are summarized in Table 1.

The observation of a stress precursor implies that low stresses are traveling at faster wave velocities than higher stresses

---

* This precursor wave is thought to result from that portion of the total wave that is transmitted through the contact points before particle rearrangement due to the total stress occurs. For this reason it would be an elastic type wave, dependent upon the character of the sand grains as well as the initial stress conditions. It is easy to see that a larger portion of the wave could be transmitted in this manner if the particles were brought into more intimate contact as a result of a high seat load.

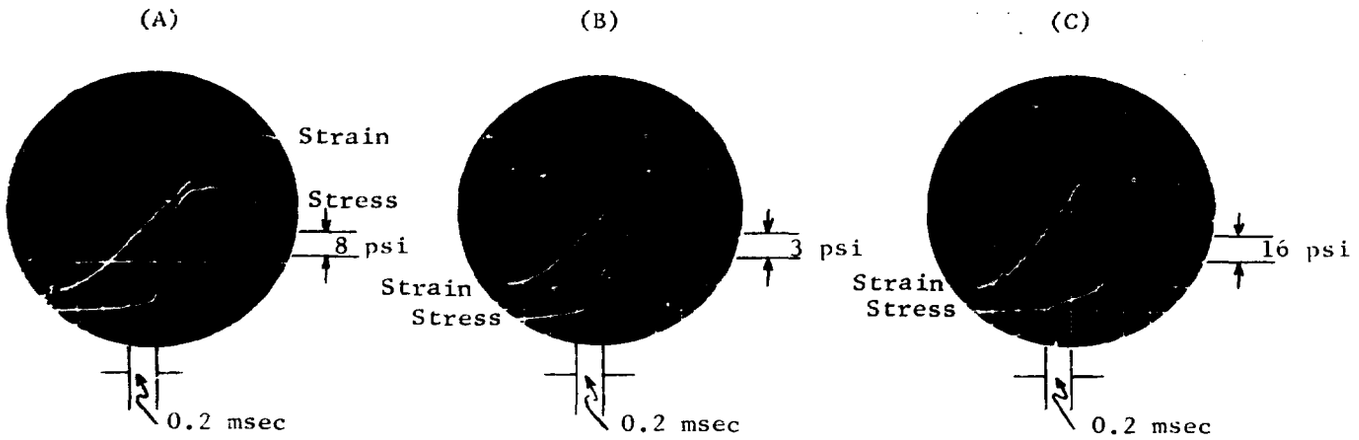


Notes:

| Static Overpressure | Dynamic Increment |
|---|---|
| (A) Zero | (A) 30 psi |
| (B) 40 psi | (B) 61 psi |
| (C) 40 psi | (C) 93 psi |

Figure 13. Oscilloscope Traces Showing a Stress Precursor in 20—30 Ottawa Sand at a Density of 110.0 pcf

Table 1

SUMMARY OF TESTS WITH INITIAL STATIC OVERPRESSURE

| | Shot Number | | |
|---|---|---|---|
| | 06016402 | 06016403 | 06016404 |
| Seat Load (psi) | 60 | 40 | 40 |
| Stress Increment (psi) | 30 | 61 | 93 |
| Initial Confining Pressure (psi) | 20 | 13 | 13 |
| Wave Velocity* (ft/sec) | 1000 | 1070 | 1070 |
| Precursor Wave Velocity** (ft/sec) | 2130 | 1780 | 1980 |
| Particle Velocity at the Middle (in./sec) | 9.3 | 27.5 | 37.0 |

*Based on time to peak incident stress.

**Based on time at which the precursor first reaches the base.

in the main wave. It has also been shown that at these higher stresses, wave velocity is proportional to the axial stress. Therefore, it is obvious that the wave velocity must decrease and then increase for increasing axial stress. Consequently, since the wave velocity is proportional to the modulus, it is readily apparent that the modulus must also decrease and then increase with stress level. This fact leads one to the conclusion that the configuration of the stress–strain curve is S-shaped.

In view of this fact, it would be a great mistake to assume a seismic wave velocity of 2000 ft/sec and a corresponding modulus of 100,000 psi for the soil, at all levels of stress, if this velocity can only be sustained under loadings of a few psi. Consequently, it may be entirely possible that seismic or vibrational velocities are limited in their usefulness for defining the modulus of soils.

Some investigators have suggested the use of constrained compression tests for the determination of the modulus near the surface and seismic or vibrational data for greater depths. The author believes that dynamic constrained compression tests are more accurate for all depths in granular materials*, provided the initial stress conditions correspond to those in the field. To rely solely on velocities obtained from applying very small stress increments would result in predicting ground motions very much smaller than what would probably occur under blast loadings.

It is possible that the precursor in cohesive soils could support a much higher level of stress, because of the bonding of particles, than was observed in the tests on sands. (Hendron and Davisson have reported a concave-downward stress – strain curve, both static and dynamic, for Frenchman Flat Playa silt to stress levels as high as several hundred psi (Ref. 6).)

---

* This modulus might be somewhat lower than the true value due to disturbance of the sample; however, with proper care, this discrepancy should not be large and it would be on the safe side.

## SOURCES OF ERROR

Better correlation, particularly in the case of particle velocity, would be desirable in that it would increase confidence in applying these results to other materials. It is believed that better correlation will be obtainable with the adaptation of the Optron 680 electro-optical trackers. This modification would allow for improved measurement of wave velocity, because two timing stations could be selected below the less constrained upper portion (2 or 3 in.) of the sample column*. Some of the uncertainties in the particle velocity measurements should also be eliminated, since the problem of inertial lag in the targets will be eliminated.

---

* The upper portion of the sample could be a source of error, since the stress wave must travel a finite distance before shocking up; most of the lateral expansion takes place in this region; and it takes a finite time to accelerate the piston up to speed.

# Section 4
# CONCLUSIONS

## CORRELATION OF MODULI

The observation of the stress precursor substantiates the postulation of an S-shaped stress–strain curve for granular materials subjected to dynamic loads. In doing so, it offers an explanation for the difference between the constrained modulus as measured in conventional compression tests and the one obtained from seismic or vibrational tests.

The correlation of moduli (obtained from the wave velocity, particle velocity, and the secant to the stress–strain curve) offers substantial evidence for allowing the use of Eqs. (1) ($M = \sigma_1/\varepsilon_1 = \rho_o C_{\sigma_1}^2 = \sigma_1^2/\rho_o v_1^2$) in predicting wave velocities and particle velocities from the stress–strain curve. In addition, a comparison with Hertzian theory shows the wave velocity increasing with stress level at a faster rate than predicted.

## Section 5
## REFERENCES

1. Zaccor, J. V. and N. R. Wallace, Techniques and Equipment for Determining Dynamic Properties of Soils, URS 155-30 for DASA Contract No. DA 49-146-XZ-019. United Research Services for the Defense Atomic Support Agency, Washington: November 1963

2. Zaccor, J. V., Techniques and Equipment for Determining Dynamic Properties of Soils, URS Interim Report 155-24 for DASA Contract No. DA 49-146-XZ-019. United Research Services for the Defense Atomic Support Agency, Washington: July 1962

3. Kaplan, K., J. Zaccor, and A. B. Willoughby, Techniques and Equipment for Determining Dynamic Properties of Soils, BRC 155-11. Broadview Research Corporation, Burlingame, California: 1960

4. Zaccor, J. V., Dynamic Behavior of Granular Media, paper presented at the Soil-Structure Interaction Symposium, University of Arizona, June 8-11, 1964

5. Deresiewicz, H., "Mechanics of Granular Matter," in Advances in Applied Mechanics, Vol. 5, Academic Press, Inc., New York: 1958, pp. 233-306

6. Hendron, A. J., Jr. and M. T. Davisson, Static and Dynamic Behavior of a Playa Silt in One-Dimensional Compression, prepared under Contract AF 29(601)-6107 and AF 29(601)-63-5577 by the University of Illinois for Air Force Weapons laboratory, 1 September 1963.
(Also published by Air Force Weapons Laboratory, Research and Technology Division, Air Force Systems Command, Project No. 1080, RTD TDR-63-3078, Kirtland Air Force Base, New Mexico, September 1963.)

7. Whitman, R. V., Nuclear Geoplosics, Part Two, "Mechanical Properties of Earth Materials," Defense Atomic Support Agency, DASA 3203 (II) Draft, Washington, D.C., June 1962

8. Whitman, R. V., Stress-Strain-Time Behavior of Soil in One-Dimensional Compression, Department of Civil Engineering, Massachusetts Institute of Technology, Report No. R63-25 for Waterways Experiment Station, May 1963, p. 19

# Appendix A
# FREE-FIELD DISPLACEMENT MEASUREMENTS

## INTRODUCTION

The attempt to make free-field measurements of any sort in soils has been universally plagued by the lack of confidence in the recorded response because the gauge embedded in the soil disturbs the free-field conditions of the medium. Also, there is still no method for calibrating these gauges that is generally accepted. Consequently, the free-field displacement system used in these tests is particularly attractive since it eliminates the need for introducing transducers into the sample itself.

## OPTRON 701 SYSTEM

A description of the theory of operation, provided by the manufacturer, is as follows (see Fig. A-1):

> The Optron is made up of a cathode ray tube (CRT), optical system, phototube, amplifier, power supply, and associated electronics. Light from the CRT spot passes through the beam splitter and is focused by a lens on the work [target]. Light is reflected off the work, diverted by the beam splitter, and is focused by the same lens in the plane of the exit slits. It passes through these slits and falls on the phototube. The output of the phototube is amplified and fed back to the CRT deflection plates. This servo loop drives the projected spot up until it reaches an edge where it locks on and remains captured to this edge. The servo keeps the spot riding

the edge with 50 percent of the spot diameter above the edge and 50 percent below. Hence, as the work moves up, the photocell tends to see more light and the servo tends to drive the spot up to regain the 50 percent above and below condition. Similarly, when the work moves down, the photocell tends to see less light and the initial bias in the servo drives the spot down to follow the motion. Hence, for any linear or complex motion, the spot is slaved or captured to the work to follow it exactly, within the frequency response of the instrument and the range capability of the lens used.

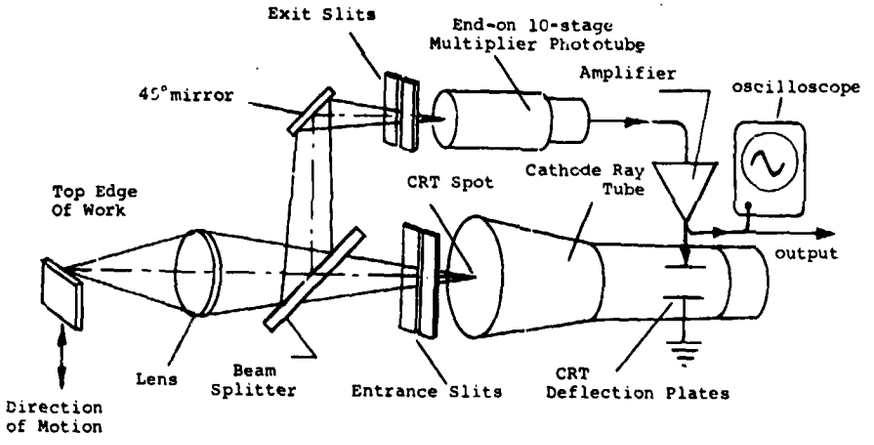


Figure A-1. Optical Layout of the Optron 701 System

Free-Field Displacement Measurements

Since the follower requires a returning light beam, targets provided by the Optron Corporation were appended to the membrane at four points along its length for use in making axial displacement measurements (Fig. 1). These targets are 1/8-in. squares of thin metal, half of which is highly reflective, while the other half is painted black.

For making lateral displacement measurements, a unique technique developed by URS is used. Four mirrors, 2 in. high by 1/4 in. wide, were mounted in the fluid annulus on either side of the column at both ends. In this technique the follower was positioned on its side, and the spot was locked on the vertical edge of the membrane. The mirror positioned behind the membrane returned half of the light beam to the instrument, the other half being absorbed or scattered by the membrane. (See Fig. A-2.) Consequently, lateral movements of the membrane caused corresponding outputs of the device.

OPTRON 680 SYSTEM

An improved device being marketed by Optron is the Model 680. The major advantage of the 680 electro-optical displacement follower for the type of testing described in this report is that it does not require a reflected light beam. The description of the principles of operation as provided by the Optron Corporation is as follows:

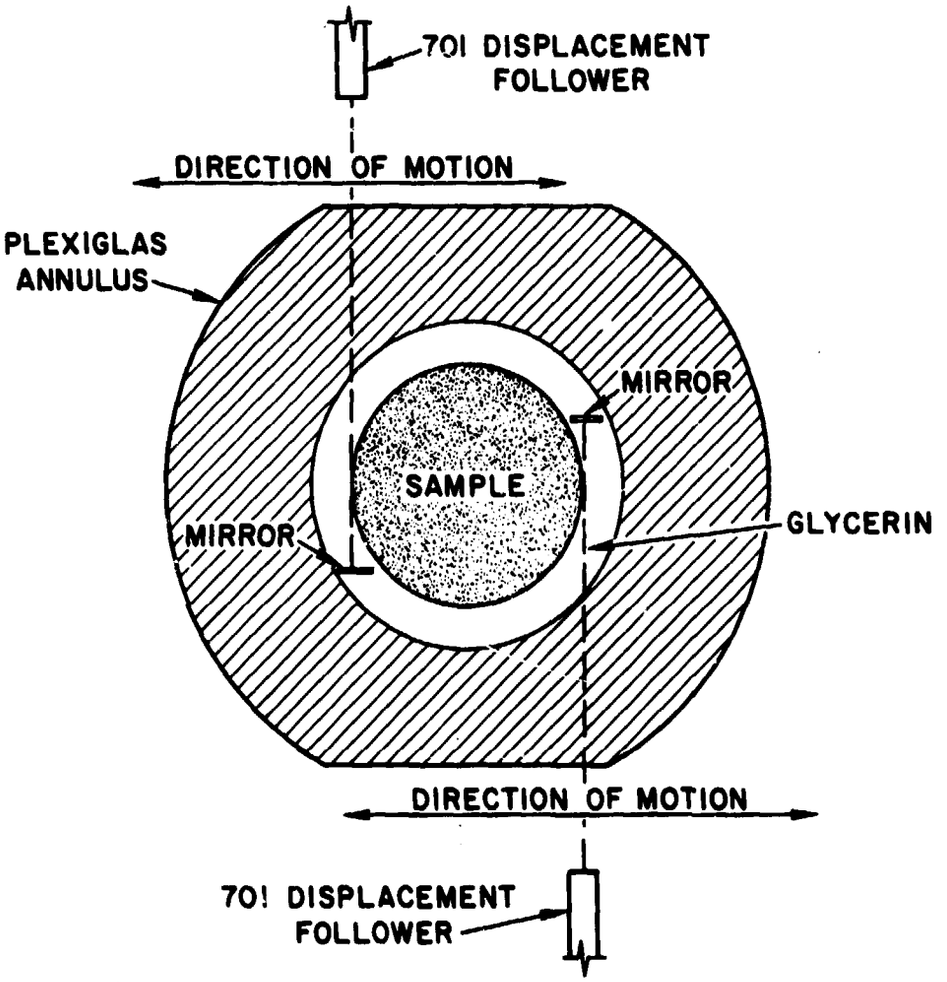


Figure A-2. Schematic of Lateral Displacement Measuring System

The image dissector tube, ID-680, is the nucleus of the system. An image is formed on the ID-680 photocathode by an optical system. This causes the cathode to emit electrons and form an electron image on the internal shield. Centrally located in this shield is a small aperture through which electrons may pass and cause a photomultiplication process to occur in the 16-stage image dissector photomultiplier section. The photomultiplier output is direct coupled to a differential amplifier which compares the output signal with a reference. The tracker is locked-on with the sharp line of contrast focused on the aperture. Any deviation from this condition causes the differential amplifier output to become unbalanced and send a correction voltage to the deflection yoke which is wrapped around the image dissector tube. The deflection yoke repositions the electron beam so that it is again centered on the aperture. Here we have a complete servo loop. A readout voltage is sampled from the differential amplifier output and, generally, is coupled to an oscilloscope or linear recorder. The only system requirement placed on the readout device is that its input impedance be greater than 100,000 ohms so as not to load down the 680 which has an output impedance of 100 ohms.

Free-Field Displacement Measurements

For application to the soil testing problem, all that is required is a reasonably sharp discontinuity in apparent brightness between two areas. Therefore, axial displacements can be measured by locking on a layer of colored sand grains*,

* If it is proven that there is no relative motion between the membrane and the sand grains, a black stripe painted on the inside of the membrane will provide a much simpler means of measuring axial displacements.

while lateral displacements can be obtained simply by locking on the edge of the membrane with the tracker positioned on its side. A few tests of this nature have been conducted demonstrating the feasibility of making such measurements. Consequently, two of these instruments have been purchased and are being installed for future testing.

# Appendix B
## SAMPLE PLACEMENT

To obtain the densities reported, one of the following methods was employed in placing the test samples. All tests were conducted on newly prepared samples, i.e., no repeat loadings were used.

### METHOD 1

This placement procedure has been described as a "raining" technique. Essentially, it consists of allowing the sand grains to fall freely from a height sufficient to permit them to attain a reasonably uniform velocity. A relatively slow rate at which the grains enter the container is required in order to obtain the optimum density. From previous studies it was concluded that this procedure would probably give the densest sample that could be obtained in this device*.

The physical process of the technique was as follows. A screen was placed across the bottom of a funnel, which was, in turn, connected to a hand-held vibrator**. A known weight of sand was placed in the funnel and the vibrator was turned on to keep the sand moving through the screen, which served to control the rate of emission.

---

* Because of the large mass of the container, it was infeasible to vibrate it as a means of increasing the sample density.

** It is manufactured by Burgess Vibrocrafters Inc. (Model V-73) and is used for engraving on metal surfaces.

This procedure was found to be very satisfactory for the placement of 20−30 Ottawa sand. It yielded a density of 110.0 pcf (RD ≃ 90%) and was found to be the most reproducible method of any that was examined, having a variation in density of about ±0.5%.

METHOD 2

The second method of sample preparation was used for obtaining densities of 105.5 pcf (RD ≃ 60%) for 20−30 Ottawa sand, 107.5 pcf (RD ≃ 80%) for Cooks Bayou sand, and 98.5 pcf (RD ≃ 70%) for the Reid Bedford Model sand. The procedure consisted of pouring one-third of the sample into the container and then vibrating it with a thin rod attached to the hand-held vibrator mentioned above. These steps were repeated until the total sample was placed. This method did not yield results that were as reproducible as those produced by the "raining" technique; however, the variation was still within about ±1%. This placement procedure produced, for the three sands tested, medium-dense samples in the range of 60−80% relative density.

## DISTRIBUTION LIST

| Item | Addresses | No. of Copies |
|---|---|---|
| 1 | Bureau of Mines, ATTN: J. E. Crawford, Washington, D.C. | 1 |
| 2 | Chief, Bureau of Yards and Docks, Department of the Navy, ATTN: Code D-440, Washington, D.C. 20370 | 1 |
| 3 | Director, Defense Atomic Support Agency, Department of Defense, ATTN: Document Library, Washington, D.C. 20301 | 5 |
| 4 | Chief of Engineers, Department of the Army, Washington, D.C. 20315 ATTN: ENGTE-E<br>ATTN: ENGMC-E | 1<br>2 |
| 5 | Chief of Naval Operations, Department of the Navy, ATTN: OP-75, Washington, D.C. 20350 | 1 |
| 6 | Chief of Research & Development, Department of the Army, ATTN: Atomic Division, Washington, D.C. 20310 | 1 |
| 7 | AFBMD, ATTN: WDFN, P.O. Box 262, Inglewood 49, California | 1 |
| 8 | Defense Documentation Center, ATTN: TISIA-21, Cameron Station, Alexandria, Virginia 22314 | 20 |
| 9 | Air Force Weapons Laboratory, Kirtland Air Force Base, New Mexico 87117 | 4 |
| 10 | Aeronautical Research Laboratory, Wright-Patterson Air Force Base, Ohio 45433 | 1 |
| 11 | Commanding General U.S. Army Materiel Command, ATTN: AMCRD-DE-N, Washington, D.C. 20310 | 3 |
| 12 | Commanding Officer and Director, U.S. Naval Civil Engineering Laboratory, Port Hueneme, California 93041 | 1 |
| 13 | Director, Weapons Systems Evaluation Group, OSD, Room 1E880, The Pentagon, Washington, D.C. 20301 | 1 |

| Item | Addresses | No. of Copies |
|---|---|---|
| 14 | Director of Civil Engineering, Headquarters, U.S. Air Force, ATTN: AFOCE, Washington, D.C. 20330 | 1 |
| 15 | Director of Defense Research & Engineering, ATTN: Technical Library, Washington, D.C. 20330 | 1 |
| 16 | Division Engineers, U.S. Army Engineer Divisions, Continental United States (1 copy to each) | 10 |
| 17 | Headquarters, U.S. Air Force, ATTN: AFTAC, C. F. Romney, Washington, D.C. 20330 | 2 |
| 18 | Director, U.S. Coast & Geodetic Survey, Department of Commerce, ATTN: D. S. Gardner, Washington, D.C. | 1 |
| 19 | Director, U.S. Coast & Geodetic Survey, Department of Commerce, ATTN: W. K. Cloud, San Francisco, California | 1 |
| 20 | U.S. Geological Survey, Department of the Interior, ATTN: J. R. Balsley, Washington, D.C. | 1 |
| 21 | California Institute of Technology, Pasadena, California ATTN: F. Press<br>ATTN: R. Benioff | 1<br>1 |
| 22 | Columbia University, ATTN: J. E. Oliver, New York New York | 1 |
| 23 | Iowa State University, ATTN: Prof. M. G. Spangler, Ames, Iowa | 1 |
| 24 | Pennsylvania State College, Atomic Defense Engineering Department, ATTN: Prof. Albright, State College, Pennsylvania | 1 |
| 25 | Barry Wright Corporation, ATTN: Mr. Cavanaugh, 700 Pleasant Street, Watertown 72, Massachusetts | 1 |
| 26 | General American Transportation Corporation, 7501 North Natchez Avenue, Niles 28, Illinois | 1 |
| 27 | Holmes & Narver, Inc., AEC Facilities Division, ATTN: Mr. Frank Galbreth, 849 S. Broadway, Los Angeles 14, California | 1 |

| Item | Addresses | No. of Copies |
|---|---|---|
| 28 | IIT Research Institute, ATTN: Library, 10 West 35th Street, Chicago 16, Illinois | 2 |
| 29 | Lawrence Radiation Laboratory, P.O. Box 808, Livermore, California | 1 |
| 30 | Space Technology Laboratories, ATTN: B. Sussholz, Inglewood, California | 1 |
| 31 | Stanford Research Institute, Physical Sciences Division, ATTN: Dr. R. B. Vaille, Jr., Menlo Park, California | 2 |
| 32 | United Research Services, ATTN: Mr. Harold G. Mason, 1811 Trousdale Drive, Burlingame, California | 20 |
| 33 | Dr. Harold Brode, RAND Corporation, 1700 Main Street, Santa Monica, California | 1 |
| 34 | Prof. John R. Hall, Jr., Department of Civil Engineering, University of Michigan, Ann Arbor, Michigan | 1 |
| 35 | Prof. B. O. Hardin, Department of Civil Engineering, University of Kentucky, Lexington, Kentucky | 1 |
| 36 | Prof. R. L. Kondner, Department of Civil Engineering, The Technological Institute, Northwestern University, Evanston, Illinois | 1 |
| 37 | Prof. Gerald A. Leonards, School of Civil Engineering, Purdue University, Lafayette, Indiana | 1 |
| 38 | Prof. N. M. Newmark, Civil Engineering Hall, University of Illinois, Urbana, Illinois 61803 | 1 |
| 39 | Prof. F. E. Richart, Jr., Department of Civil Engineering, The University of Michigan, Ann Arbor, Michigan 48104 | 1 |
| 40 | Prof. John H. Schmertmann, Civil Engineering Department, University of Florida, Gainsville, Florida | 1 |
| 41 | Prof. H. Bolton Seed, Department of Civil Engineering, University of California, Berkeley, California | 1 |

| Item | Addresses | No. of Copies |
|---|---|---|
| 42 | Prof. H. Neils Thompson, Civil Engineering Department, University of Texas, Austin 12, Texas | 1 |
| 43 | Prof. L. J. Thompson, Department of Civil Engineering, University of New Mexico, Albuquerque, New Mexico | 1 |
| 44 | Prof. R. V. Whitman, Department of Civil Engineering, Massachusetts Institute of Technology, Cambridge 39, Massachusetts | 1 |
| 45 | Mr. C. J. Nuttall; Wilson, Nuttall, Raimond Engineers, Inc.; Chestertown, Maryland | 1 |
| 46 | Mr. W. R. Perret, 5112 Sandia Corporation, Sandia Base, Albuquerque, New Mexico | 1 |
| 47 | Dr. Grover L. Rogers, RECON, Inc., Box 3622 MSS, Tallahassee, Florida | 1 |
| 48 | Mr. Fred Sauer, Physics Department, Stanford Research Institute, Menlo Park, California | 1 |
| 49 | Mr. A. A. Thompson, Terminal Ballistics Laboratory, Aberdeen Proving Ground, Aberdeen, Maryland | 1 |

Unclassified

Security Classification

**DOCUMENT CONTROL DATA - R&D**

*(Security classification of title, body of abstract and indexing annotation must be entered when the overall report is classified)*

1 ORIGINATING ACTIVITY (Corporate author):
United Research Services, Inc.
Burlingame, California

2a REPORT SECURITY CLASSIFICATION
Unclassified

2b GROUP

3 REPORT TITLE STUDY OF THE DYNAMIC STRESS-STRAIN AND WAVE-PROPAGATION CHARACTERISTICS OF SOILS: Report 2, CORRELATION OF STRESS-STRAIN AND WAVE-PROPAGATION PARAMETERS IN SHOCK-LOADING DRY SALTS

4 DESCRIPTIVE NOTES (Type of report and inclusive dates)
Report 2 of series

5 AUTHOR(S) (Last name, first name, initial)
Durbin, William L.

| 6 REPORT DATE | 7a TOTAL NO OF PAGES | 7b NO OF REFS |
|---|---|---|
| November 1961 | 51 | 8 |

| 8a CONTRACT OR GRANT NO | 9a ORIGINATOR'S REPORT NUMBER(S) |
|---|---|
| Contract No. DA-22-079-eng-373 | URS 637-15 |
| b PROJECT NO | |
| c | 9b OTHER REPORT NO(S) (Any other numbers that may be assigned this report) |
| d | Waterways Experiment Station Contract Report No. 3-91 |

10 AVAILABILITY LIMITATION NOTICES
Qualified requesters may obtain copies of this report from DDC

| 11 SUPPLEMENTARY NOTES | 12 SPONSORING MILITARY ACTIVITY |
|---|---|
| Project funded by Defense Atomic Support Agency | U.S.Army Engineer Waterways Experiment Station, CE, Vicksburg, Miss. |

13 ABSTRACT Wave propagation studies conducted on laterally confined columns of three granular materials which exhibit nonlinear stress-strain behavior are described. Under these conditions, axial and lateral stresses and strains, wave velocities, and particle velocities measured at points along the column are reported. A new technique for measuring free-field displacements without physically contacting the soil is also described.

A correlation between the moduli computed from the stress wave velocity, particle velocity, and the account drawn to the stress-strain curve is presented. Relationships between stress, strain, wave velocity, and particle velocity are shown to be such that if any two of the parameters are known, the other two may be determined. Comparison of the data is made with H. Hertz's theory relating normal stress to wave velocity or confining pressure.

The difference between a stress-strain curve for a shock front and the unique relationship that exists between stress and strain for shock loading is presented.

Correlations are presented showing relationships between radial stress and strain rates taken after passage of the incident wave and those taken after the passage of the reflected wave.

Several interesting though preliminary observations on stress precursors resulting from initial axial stresses are presented. From these observations, an explanation is presented for the disparity between moduli based on unconfined compression tests and those back-figured from elastic velocities.

DD FORM 1473

Unclassified

Security Classification

Unclassified
Security Classification

| 14 KEY WORDS | LINK A | | LINK B | | LINK C | |
|---|---|---|---|---|---|---|
| | ROLE | WT | ROLE | WT | ROLE | WT |
| Sand | | | | | | |
| Shock waves | | | | | | |
| Soils--Stress | | | | | | |
| Soils--Wave transmission | | | | | | |

INSTRUCTIONS

1. ORIGINATING ACTIVITY: Enter the name and address of the contractor, subcontractor, grantee, Department of Defense activity or other organization *(corporate author)* issuing the report.

2a. REPORT SECURITY CLASSIFICATION: Enter the overall security classification of the report. Indicate whether "Restricted Data" is included. Marking is to be in accordance with appropriate security regulations.

2b. GROUP: Automatic downgrading is specified in DoD Directive 5200.10 and Armed Forces Industrial Manual. Enter the group number. Also, when applicable, show that optional markings have been used for Group 3 and Group 4 as authorized.

3. REPORT TITLE: Enter the complete report title in all capital letters. Titles in all cases should be unclassified. If a meaningful title cannot be selected without classification, show title classification in all capitals in parenthesis immediately following the title.

4. DESCRIPTIVE NOTES: If appropriate, enter the type of report, e.g., interim, progress, summary, annual, or final. Give the inclusive dates when a specific reporting period is covered.

5. AUTHOR(S): Enter the name(s) of author(s) as shown on or in the report. Enter last name, first name, middle initial. If military, show rank and branch of service. The name of the principal author is an absolute minimum requirement.

6. REPORT DATE: Enter the date of the report as day, month, year; or month, year. If more than one date appears on the report, use date of publication.

7a. TOTAL NUMBER OF PAGES: The total page count should follow normal pagination procedures, i.e., enter the number of pages containing information.

7b. NUMBER OF REFERENCES: Enter the total number of references cited in the report.

8a. CONTRACT OR GRANT NUMBER: If appropriate, enter the applicable number of the contract or grant under which the report was written.

8b, 8c, & 8d. PROJECT NUMBER: Enter the appropriate military department identification, such as project number, subproject number, system numbers, task number, etc.

9a. ORIGINATOR'S REPORT NUMBER(S): Enter the official report number by which the document will be identified and controlled by the originating activity. This number must be unique to this report.

9b. OTHER REPORT NUMBER(S): If the report has been assigned any other report numbers *(either by the originator or by the sponsor)*, also enter this number(s).

10. AVAILABILITY/LIMITATION NOTICES: Enter any limitations on further dissemination of the report, other than those imposed by security classification, using standard statements such as:

(1) "Qualified requesters may obtain copies of this report from DDC."

(2) "Foreign announcement and dissemination of this report by DDC is not authorized."

(3) "U. S. Government agencies may obtain copies of this report directly from DDC. Other qualified DDC users shall request through _____."

(4) "U. S. military agencies may obtain copies of this report directly from DDC. Other qualified users shall request through _____."

(5) "All distribution of this report is controlled. Qualified DDC users shall request through _____."

If the report has been furnished to the Office of Technical Services, Department of Commerce, for sale to the public, indicate this fact and enter the price, if known.

11. SUPPLEMENTARY NOTES: Use for additional explanatory notes.

12. SPONSORING MILITARY ACTIVITY: Enter the name of the departmental project office or laboratory sponsoring *(pay for)* the research and development. Include address.

13. ABSTRACT: Enter an abstract giving a brief and factual summary of the document indicative of the report, even though it may also appear elsewhere in the body of the technical report. If additional space is required, a continuation sheet shall be attached.

It is highly desirable that the abstract of classified reports be unclassified. Each paragraph of the abstract shall end with an indication of the military security classification of the information in the paragraph, represented as (TS), (S), (C), or (U).

There is no limitation on the length of the abstract. However, the suggested length is from 150 to 225 words.

14. KEY WORDS: Key words are technically meaningful terms or short phrases that characterize a report and may be used as index entries for cataloging the report. Key words must be selected so that no security classification is required. Identifiers, such as equipment model designation, trade name, military project code name, geographic location, may be used as key words but will be followed by an indication of technical context. The assignment of links, rules, and weights is optional.

Unclassified
Security Classification